Preoperative localization of parathyroid glands

Use of MRI, scintigraphy, and image fusion

J. Ruf[1], E. Lopez Hänninen[1], Th. Steinmüller[2], T. Rohlfing[3], H. Bertram[1], M. Gutberlet[1], A.-J. Lemke[1], R. Felix[1], H. Amthauer[1]

Department of [1]Radiology and Nuclear Medicine [2]Visceral and Transplant Surgery, Charité, Universitätsmedizin Berlin, Campus Virchow Clinic, Germany

[3]Image Guidance Laboratories, Department of Neurosurgery, Stanford University, USA

Präoperative Lokalisationsdiagnostik von Nebenschilddrüsen: Nutzen der MRT, Szintigraphie und Bildfusion

Keywords
Parathyroid gland, adenoma, scintigraphy, magnetic resonance imaging, image fusion

Summary
Aim: Minimally invasive resection of hyperfunctional parathyroid glands is an alternative to open surgery. However, it requires a precise preoperative localization. This study evaluated the diagnostic use of magnetic resonance (MR) imaging, parathyroid scintigraphy, and consecutive image fusion. **Patients, methods:** 17 patients (9 women, 8 men; age: 29-72 years; mean: 51.2 years) with primary hyperparathyroidism were included. Examination by MRI used unenhanced T1- and T2-weighted sequences as well as contrast-enhanced T1-weighted sequences. ^{99m}Tc-MIBI scintigraphy consisted of planar and SPECT (single photon emission tomography) imaging techniques. In order to improve the anatomical localization of a scintigraphic focus, SPECT-data were fused with the corresponding MR-data using a modified version of the Express 5.0 software (Advanced Visual Systems, Waltham, MA). Results of image fusion were then compared to histopathology. **Results:** In 14/17 patients, a single parathyroid adenoma was found. There were 3 cases with hyperplastic glands. MRI detected 10 (71%), scintigraphy 12 (86%) adenomas. Both modalities detected 1/3 patients with hyperplasia. Image fusion improved the anatomical assignment of the 13 scintigraphic foci in five patients and was helpful in the interpretation of inconclusive MR-findings in two patients. **Conclusions:** Both MRI and ^{99m}Tc-MIBI scintigraphy sensitively detect parathyroid adenomas but are less reliable in case of hyperplastic glands. In case of a scintigraphic focus, image fusion considerably improves its topographic assignment. Furthermore, it facilitates the evaluation of inconclusive MRI findings.

Schlüsselwörter
Nebenschilddrüsenadenom, Bildfusion

Zusammenfassung
Ziel: Die minimal-invasive Resektion hypersezernierender Nebenschilddrüsen ist eine Alternative zur offenen Chirurgie, bedarf jedoch einer präzisen präoperativen Lokalisationsdiagnostik. Diese Studie evaluierte den Nutzen von Magnetresonanztomographie (MRT), Nebenschilddrüsenszintigraphie und konsekutiver Bildfusion. **Patienten, Methoden:** 17 Patienten (9 Frauen, 8 Männer, Alter: 29-72 Jahre; Mittel: 51,2 Jahre) mit primärem Hyperparathyreoidismus wurden in diese Studie eingeschlossen. Die MRT-Untersuchung umfasste T2- und T1-gewichtete Sequenzen. Die ^{99m}Tc-MIBI-Szintigraphie wurde in planarer und SPECT(single photon emission tomography)-Technik durchgeführt. Zur Verbesserung der anatomischen Zuordnung eines szintigraphischen Fokus, wurden die SPECT-Daten mit dem korrespondierenden MRT-Datensatz fusioniert. Hierfür wurde eine modifizierte Version der Software Express 5.0 (Advanced Visual Systems, Waltham, MA) verwendet. Die Ergebnisse der Bildfusion wurden mit den histopathologischen Befunden verglichen. **Ergebnisse:** Bei 14 Patienten wurde ein singuläres Nebenschilddrüsenadenom nachgewiesen. Bei 3 Patienten wurden hyperplastische Drüsen entdeckt. Die MRT entdeckte 10 (71%) und die Szintigraphie 12 (86%) der Adenome. Beide Verfahren detektierten hyperplastische Drüsen in einem von drei Fällen. Die Bildfusion verbesserte die anatomische Zuordnung der 13 szintigraphischen Foki bei 5 Patienten und war bei 2 Patienten für die Interpretation uneindeutiger MRT-Befunde von Nutzen. **Schlussfolgerung:** Während Adenome der Nebenschilddrüse sowohl mit der MRT als auch mit der ^{99m}Tc-MIBI-Szintigraphie zuverlässig nachgewiesen werden, ist die Detektion hyperplastischer Drüsen mit beiden Verfahren weniger sensitiv. Im Falle eines szintigraphischen Fokus verbessert die Bildfusion in hohem Maße seine topographische Zuordnung. Darüber hinaus erleichtert sie die Interpretation nicht eindeutiger MRT-Befunde.

Nuklearmedizin 2004; 43: 85–90

Single adenomas of the parathyroid gland are the most frequent cause (approx. 85%) of hyperparathyroidism. To a lesser extent (up to 15%), multiple adenomas and hyperplastic glands and in rare cases carcinomas (<1%) are responsible for glandular hyperfunction (21). Surgical resection is the therapy of choice and offers a cure for non-malignant disease in more than 95% of all cases (26). Although the traditional approach for parathyroidectomy (open cervicotomy and bilateral neck exploration) yields very good results in the hands of the experienced endocrine surgeon (3), new procedures such as unilateral open or minimal invasive techniques are getting more common, as they appear to reduce operation time, hospital stay and complication rate while improving cosmetic results (37). However, these methods require the preoperative localization of the pathologically altered gland(s). Morphological imaging includes high resolution ultrasound (US) that is a meanwhile almost ubiquitous available method with a sensitivity of up to 65-90%, (5, 22, 29, 33, 38). However, especially ectopic glands can be difficult to detect, particularly if they are located behind the larynx, clavicle or in the mediastinum (1). The detection of adenomas by magnetic resonance imaging (MRI) is reported to have a sensitivity of 62.5-94% and a specificity of 75-88% (17, 18) and seems to be more suitable than computed tomography (CT), which has a sensitivity of only 40-44% and a specifity of up to 88% (12, 39). On the other hand, functional imaging approaches with parathyroid scintigraphy are widely used. Parathyroid scintigraphy with the tracer Tc-99m-MIBI (Tc-MIBI), mainly done in dual-phase technique,

Eingegangen: 10. Oktober 2003; in revidierter Form: 3. Dezember 2003

appears to be superior to Tl-201-Tc-99m-pertechnetate subtraction scintigraphy, achieving sensitivities of 68-95% and specificities of 75-100% (3, 12, 16, 17, 22-26, 29, 33, 35). Although the subtraction technique also delivers excellent results when applied to Tc-99m-MIBI scanning, the dual-phase technique remains popular as it is technically less demanding (5). The use of single photon emission tomography (SPECT) seems to further improve sensitivity (23-25). In addition to technical improvements, other tracers like Tc-99m-Tetrofosmin are under evaluation (38).

However, concomitant thyroid nodules reduce the sensitivity of all modalities (US: 47-53%, MRI: 75%, Tc-MIBI: 68-73% (15, 24, 29, 34) and all techniques have shown a lower accuracy for the detection of multiple adenomas or hyperplastic disease (sensitivity US: 48%, MRI: 54-75%, Tc-MIBI: 37-64%. (3, 17, 18, 26, 38) as well as secondary hyperparathyroidism (36).

Sensitivity can be improved by the combination of examinations, preferably morphological and functional imaging, as has been shown for US and Tc-MIBI scintigraphy (15, 33). Such visual comparative analysis is commonplace in clinical routine. However, the accuracy "mental fusion" is limited (13). As this correlation is often insufficient for complex and/or small anatomical regions, there have been many attempts to create a single system of reference. These techniques can be both prospective (e.g. stereotactic frames, fiducial markers) or retrospective in nature (e.g. manual co-registration or mathematical correlations based on surface or voxel information). Experience on image fusion using CT, MRI, SPECT or PET data has mainly been gained in brain examination studies (13, 20, 40). It has been shown that retrospective registration of CT- and SPECT-data by voxel-based algorithms is a very reliable approach when compared to the prospective "gold-standard" of stereotactic frames (42). This technique is based on normalized mutual information which assigns a geometric function between two images based on the degree of similarity of voxel-information between the two sets of data to be matched. Maximization describes the use of algorithms that reduce the difference in information between a voxel and its attributed match to a minimum for all voxel-pairs (19, 27). The result of this co-registration can be visualized as a fused image of both modalities.

For the detection of adenomas of the parathyroid gland, we performed both MR and Tc-MIBI imaging in patients with parathyroid pathology. Each single modality was evaluated independently, in combination and after image fusion.

Patients and methods

Seventeen patients with primary hyperparathyroidism were included in this study (9 female, 8 male, age ranging from 29 to 72 years, the mean age being: 52.2 years). All patients were fully evaluable.

^{99m}Tc-MIBI scintigraphy and magnetic resonance imaging

Both examinations were performed within 0-9 days (mean 2.5 days) in each patient.

Scintigraphy was performed by intravenously injecting 500-600 MBq ^{99m}Tc-MIBI (Cardiolite®, Bristol-Myers Squibb GmbH, Munich, Germany). Planar images of the neck and thorax region were acquired 20 minutes (early) and 1.5 hours (late) p.i. using a 64 × 64 matrix with a LEHR-collimator (SP4 Elscint, GE Medical Systems, Solingen, Germany). After the late scan, SPECT imaging was performed with a 3-head gamma camera using a 128 × 128 matrix and LEHR-collimators (Multispect, Siemens, Erlangen, Germany); the acquisition time was 30 seconds at 60 stops. Detection of a focus, especially in the late scan was considered to be a positive finding.

Magnetic resonance imaging used an anterior neck surface coil in a 1.5 T unit (Magnetom SP63, Siemens, Erlangen, Germany; Gyroscan ACS-NT, Philips, Best,

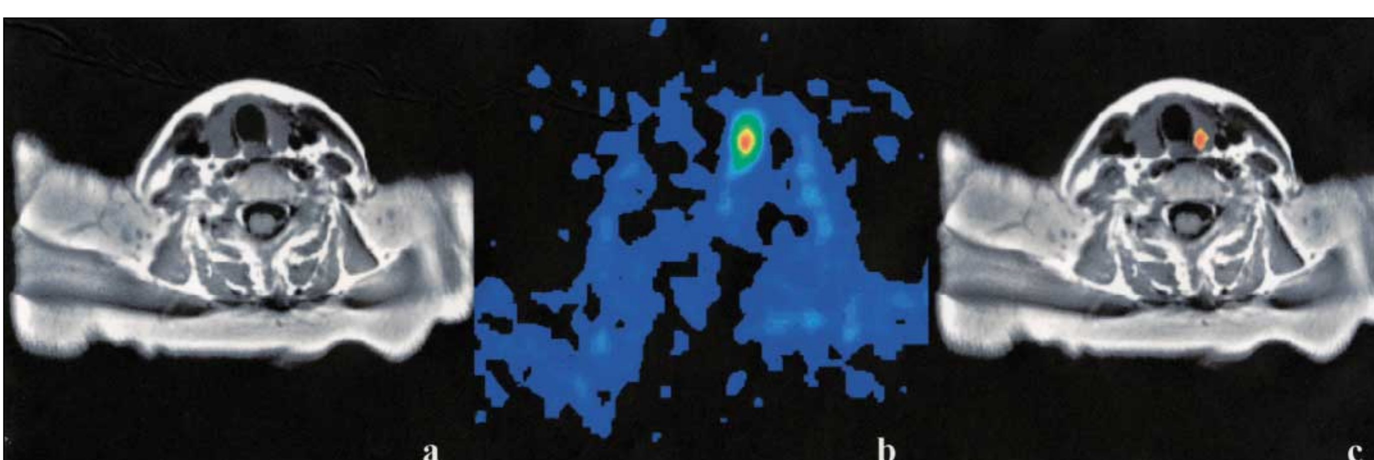

Fig. 1 T1-weighted transversal MR-images (a), transversal reconstruction of SPECT data acquired 1.5 hours p.i. (b)
Visualization of the corresponding MRI- (a) and SPECT-data (b) in one set of images (c) is possible after voxel-based co-registration by maximized mutual information.

Tab. 1 Imaging results and histopathology
(pat.: patient, m: man, f: woman, yrs.: years, Pth: parathyroid, OP: operation, histo.: histopathology, H: hyperplasia, A: adenoma, n.d.: not done, OP: operation, #: number of resected glands, MIV: minimally invasive video-assisted, *: additional thyroid operation)

pat.	sex	age yrs.	previous OP PTh (#)	previous OP thyroid	histo (#)	weight (mg)	positive imaging MRI	positive imaging SPECT	image fusion:result	localisation	operation
1	f	35	yes (3)	no	H (1)	2300	no	yes	improved localization	right sterno-clavicular joint	unilateral
2	f	65	no	no	A (1)	3000	yes	yes	no additional information	cranial right	unilateral
3	m	69	no	no	A (1)	1800	yes	no	not applicable	paratracheal right	unilateral
4	f	29	no	no	A (1)	800	yes	yes	no additional information	paraoesophagal left	unilateral MIV
5	f	49	no	no	A (1)	1000	yes	yes	differentation from lymphnode	caudal left	unilateral MIV
6	f	56	no	no	H (1)	400	yes	no	not applicable	caudal right	unilateral*
7	m	30	no	no	A (1)	5000	yes	yes	no additional information	caudal right	bilateral
8	m	48	no	no	H (3)	n.d	no	no	not applicable	orthotopic (2x left, 1x right)	bilateral*
9	f	69	no	no	A (1)	600	yes	yes	differentation from nerve ganglion	caudal left	unilateral
10	m	44	no	no	A (1)	1000	yes	no	not applicable	caudal left	uni→bilat.
11	m	58	no	no	A (1)	400	no	yes	improved localization	caudal left	bilateral
12	f	40	no	no	A (1)	300	no	yes	improved localization	caudal left	unilateral
13	m	64	no	no	A (1)	800	no	yes	improved localization	cranial left	unilateral
14	m	53	no	yes	A (1)	5500	yes	yes	no additional information	caudal right	unilateral
15	m	24	no	no	A (1)	11800	yes	yes	no additional information	caudal left	bilateral*
16	f	65	no	no	A (1)	750	no	yes	improved localization	caudal left	unilateral
17	f	72	no	no	A (1)	400	yes	yes	no additional information	caudal right	unilateral MIV

The Netherlands). Both T1- and T2-weighted spin-echo sequences were acquired and T1-weighted sequences were repeated after the i.v. administration of gadopentetate dimeglumine (Magnevist®, Schering AG, Berlin, Germany) at 0.2 mmol/kg body-weight. Slice thickness was 4 mm (transversal and coronal orientation) and the field of view was 12 to 15 cm, the matrix 256 × 256. The same sequences were used for upper thorax imaging (slice thickness was 5 mm, field of view 16 to 18 cm, and the matrix was 192 × 256). A positive finding was characterized by a hyperintensive signal in T2 while showing an increase of signal-intensity in T1 after intravenous application of the contrast medium.

Registration and image fusion

For co-registration of MRI- and SPECT-data and consecutive image fusion (Fig. 1), we used a modified version of AVS/Express 5.0 (Advanced Visual Systems, Waltham, MA, U.S.A.) on an O2-Workstation (Silicon Graphics, Mountain View, Ca/USA). Transferal of image data to the workstation was done by intranet.

Image fusion was subdivided into three steps. The first step included the correction of inhomogeneities, the correction of spatial orientation as well as the assimilation of matrix sizes for both modalities. The initial co-registration according to internal landmarks (e.g. surface outlines) was performed manually, adjusting translation- and rotation-parameters in all three dimensions in order to achieve a rough congruency between the two sets of images followed by the software's voxel-based registration algorithm. This so called "maximal" registration, uses the concept of normalized mutual information, then "fine tuned" the fusion of the volume-data. Here, minute rotations and translations were performed, using the degree of similarity between the corresponding paired voxels of each set of volume-data as a measure (19). Additionally, coincidence thresholding was performed as it greatly reduced computation time and improved performance by reducing background noise in SPECT-data (30). All results were subject to visual plausibility control.

Results

Surgery was performed in all 17 patients. Initially, 11 patients underwent unilateral parathyroidectomy (3 minimally invasive). In one patient, the unilateral exploration had to be expanded into a bilateral operation. Five patients primarily underwent bilateral cervical exploration. One patient with prior hemithyroidectomy also received a resection of a nodule in the remaining lobe. Moreover, three other patients underwent additional hemithyroidectomy due to singular thyroid nodules. All imaging findings were verified by postoperative histopathology.

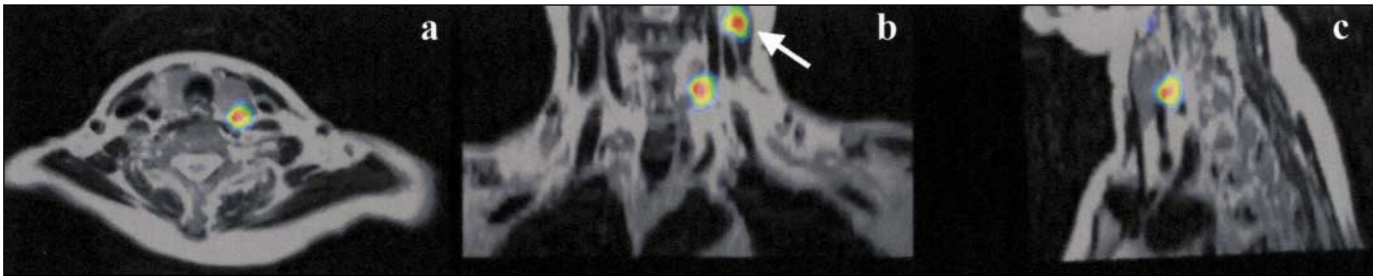

Fig. 2 Woman (age: 40 years) with primary hyperparathyreoidism: fused images localize the adenoma behind the lower pole of the left thyroid lobe in the axial (a), coronal (b), and sagittal (c) reconstructions (arrow: focus of unspecific asymmetric tracer accumulation in the left parotid gland)
Note that the breathing artifacts in the MR-data-set posed no difficulties for the computation algorithm.

Histology showed a singular adenoma of the parathyroid gland in 14/17 patients. 2/17 patients had uniglandular hyperplasia, in one patient, three glands were affected. Adenomas weighted between 300 and 11800 mg (mean: 2368 mg), singular hyperplastic glands weighted 300, 400 and 2300 mg. The weight of the one case with multiple hyperplastic glands was not determined.

Preoperatively, MRI detected 10/14 (71%) and scintigraphy 12/14 (86%) of all adenomas. Furthermore, there were two additional false positives in MR-imaging (1 lymph node and 1 nerve ganglion) that were not classified as pathologic in scintigraphy (Tab. 1).

Both examinations detected 1/3 singular hyperplasias. In the one patient with multiple hyperplastic glands neither modality detected any pathology.

Image fusion was successfully performed in all 13 patients with positive scintigraphic findings. Diagnostic improval was observed in 7 (54%) of these 13 patients. Thus in 5/13 (38%) patients, image fusion resulted in an improved topographic assignment of scintigraphic foci (Fig. 2). In 2 (15%) patients it helped to differentiate hyperactive parathyroid tissue from neighboring lymph nodes (n = 1) or a nerve-ganglion (n = 1). In the remaining six patients, image fusion had no impact on the clinical treatment strategy (Tab. 1). Due to the small number of patients in this study, only descriptive statistical analysis was performed.

Discussion

The role of imaging studies for the detection of adenomas of the parathyroid gland before surgery is still being discussed controversially, however it permits the use of unilateral and/or minimally invasive surgery that appears to be equally efficient while reducing operation time, complication rates, and patient morbidity and, furthermore, cutting down costs (37).

Ultrasound is a very sensitive modality for the detection of adenomas of the parathyroid gland (5, 22, 29, 33, 38) and due to its widespread use and availability it is considered to be the first modality prior to surgery (22). It is, however, very user-dependent and the results are difficult to reproduce, furthermore ectopic mediastinal glands that are observed in about 10-20% of all cases (1) cannot be detected.

MRI has also been proven to be very useful for the detection of adenomas, especially in case of ectopic mediastinal localization. In sensitivity and specifity it appears to be superior to CT which is sometimes troubled by streak artifacts in the shoulder region apart from exposing the patient to radiation (7, 12, 17, 39). In a previous study, good results using MRI have been demonstrated (18). Employing the same protocol, MRI detected 71% of 14 adenomas in this study. However, consistent with previous studies, the detection of hyperplastic glands was less reliable (17, 38). Apart from glandular size, signal intensity and contrast enhancement seem to be influenced by cellular composition, i.e. fibrosis or haemorrhage (2).

Scintigraphic detection of the parathyroid adenomas by Tc-MIBI using dual phase technique is considered to be a very sensitive and specific imaging approach (3, 17). Although Tc-MIBI-scintigraphy is reliable in the detection of adenomas larger than 500 mg (3), our results (Tab. 1) and the results of other studies show that the detection of smaller adenomas is frequently possible and large adenomas (>1 g) are often not detected (25, 38). This emphasizes the fact that tracer accumulation is not merely based on size alone, but also to some extent on the degree of hyperfunction which in turn is thought to be represented by the mitochondrial content (9). Accordingly, the lesser sensitivity of Tc-MIBI in case of hyperplastic glands might not only be caused due to smaller size but also due to a lower mitochondrial hyperfunction in the more heterogeneous, often polyclonatic hyperplasias (36). Furthermore, as in MRI contrast-enhancement, determination of the size or mass of a given gland often does not reflect the heterogeneous cellular tissue composition as opposed to the, mainly oxyphil, mitochondria-rich cells fatty tissue or necrosis shows no tracer accumulation (35). Accordingly, nonfunctional tissue contributed to a large part to the total glandular size in both false-negative adenomas (Tab. 1). Finally, it must be noted that additional factors such as P-glycoprotein or MDR (multi drug resistance) protein expression are held responsible for nuclide accumulation (28).

As small adenomas (or large adenomas with a small functional compound) with their relatively low uptake might still be hidden behind structures with physiological nuclide accumulation, i.e. thyroid tissue in planar images, additional SPECT-imaging is often performed. One advantage clearly lies in the improved differentiation between thyroid/parathyroid tracer uptake and especially in the topographical assignment of ectopic foci (7). However, the improvement of sensitivity by SPECT-imaging is still seen somewhat controversial: while Staudenherz et al. (34) did not perceive a clear benefit for sensitivity, studies by Moka et al. postulate an increase of sensitivity of up to 24% (23-25). Although high sensitivities (95-96%) were thus achieved for the lateralization of adenomas, the actual topographical assignment of foci, crucial for minimal invasive procedures, was less sensitive (approx. 80%). The group also performed 3D-reconstructions of SPECT-data for anatomical localization, but even this approach does not compensate the drawback of the functional imaging approach, i.e. the lack of information on surrounding tissue for anatomical orientation.

Therefore, scintigraphic findings are frequently visually correlated with ultrasound and MR or CT imaging. Although this correlation often proves to be sufficient, it is limited by the accuracy of mental image fusion (13). Furthermore, the presence of concomitant goiter nodules, which may be observed in 30% of all patients with hyperparathyroidism in central Europe (7), does not only adversely affect the detection of adenomas in Tc-MIBI-scintigraphy (3, 22, 24, 26, 29) and in morphological imaging (15, 17, 22, 29), but also in the consecutive mental correlation of findings. Therefore we performed image fusion of MR- and MIBI-SPECT-data as both examinations allow the detection of ectopic mediastinal adenomas and generate the volume data necessary for image fusion.

Experience in image fusion is largely based on head examinations (20). However, brain imaging is very favorable for image fusion techniques few motions occur in the relatively rigid "scalp-skull-brain" system whose anatomy facilitates the use of stereotactic techniques. In contrast, the cervical region is subject to motion and positioning artifacts and invasive measures like stereotactic frames are not feasible. Alternatively, non-invasive prospective approaches such as fiducial marker-based coordinate systems (40) could be used. However, the preparation of the patients in the pre-acquisition phase is often time consuming (13). An alternative to these prospective techniques is retrospective image fusion by voxel-based algorithms. Although these algorithms have been proved to be very accurate in rigid body settings (19, 27, 42), motion artifacts (troubling even SPECT-CT systems) will influence the result in other regions (6). Thus, the positioning of the patient in both examinations remained a crucial element in this study and all fusion images were subject to visual plausibility control. If necessary, they were manually corrected, using thyroid or background activity as "internal landmarks". Despite these limitations, the image fusion approach described herein has already been successfully used for other clinical non-head examinations (10, 11).

Rubello et al. (31) reported the use of image fusion for the detection of an ectopic adenoma. In contrast to our study however, CT-data were used for anatomical information. Due to our experience (18), we only employ CT if there is a contraindication for MRI examination (e.g. pacemakers).

As mentioned, hybrid systems are currently considered to be the gold-standard of image fusion (13) and have also successfully been used for the detection of adenomas of the parathyroid gland (6). With the hybrid-approach as well, the benefit of fused imaging for the detection of ectopic glands located in the mediastinum was demonstrated (14). However, aside from the higher costs of these SPECT-CT-systems, a major drawback is the morphological imaging component, the low-resolution rotating x-ray-tube. Its fused images do provide basic anatomical orientation, but in contrast to our retrospective image fusion method, the morphological component has a low diagnostic quality. Our image fusion technique does not only allow the anatomical assignment of scintigraphic foci, it also provides the full potential MRI offers for the detection of adenomas. Thus, we observed a diagnostic benefit in 54% of those patients analyzed with image fusion.

It cannot be denied that for routine preoperative examinations, MIBI-scintigraphy in conjunction with ultrasound forms a reliable combination for the detection of adenomas in loco typico. Even more important, the combination with ultrasound is surely more cost-efficient than with our MR-approach (41). Although we observed no ectopic parathyroid adenomas in our patient population, it has to be pointed out that this study mainly served as a validation process for our method. Instead of routine examinations, we do see its value mainly in the improved detection of ectopic glands when the performance of ultrasound is simply not feasible and the higher costs of MR are justified. As demonstrated above, image fusion has been shown to be very promising for the precise localization of thoracal adenomas (14, 31) and, as discussed above, we do expect a further improval if MR instead of CT is used as the morphological component. Furthermore, another indication for this technique is seen in the detection of pathologic findings in persistent hyperparathyroidism, where fibrosis of previous interventions limits not only ultrasound but also cervical exploration (8). In this aspect, it might also complement minimal invasive gamma-probe guided approaches (4).

Conclusion

Both MR-imaging and ^{99m}Tc-MIBI scintigraphy are sensitive methods for the detection of adenomas of the parathyroid gland but are less reliable in the localization of hyperplastic glands. Retrospectively generated fused images from MR- and SPECT-data considerably enhance the topographic assignment of scintigraphic foci. As the MR-component itself allows a characterization of parathyroid tissue an improved localization and/or exclusion of ectopic glands can be achieved. Consequently, improved preoperative imaging might reduce the rate of bilateral cervical exploration, paving the way to minimally invasive or at least unilateral surgical approaches.

Acknowledgements
This study was supported by Deutsche Forschungsgemeinschaft as part of the project Graduiertenkolleg 331 "Temperaturabhängige Effekte in Therapie und Diagnostik" (Grant No. GRK331-1/97). TR was supported by the National Science Foundation (USA) under Grant No. EIA-0104114.

References

1. Akerstrom G, Malmaeus J, Bergstrom R. Surgical anatomy of human parathyroid glands. Surgery 1984; 95: 14-21.
2. Auffermann W, Guis M, Tavares NJ et al. MR signal intensity of parathyroid adenomas: correlation with histopathology. Am J Roentgenol 1989; 153: 873-6.
3. Caixas A, Berna L, Hernandez A et al. Efficacy of preoperative diagnostic imaging localization of technetium 99m-sestamibi scintigraphy in hyperparathyroidism. Surgery 1997; 121: 535-41.
4. Casara D, Rubello D, Pelizzo MR et al. Clinical role of $^{99m}TcO_4$/MIBI scan, ultrasound and intra-operative gamma probe in the performance of unilateral and minimally invasive surgery in primary hyperparathyroidism. Eur J Nucl Med 2001; 28: 1351-9.
5. Coakley AJ. Parathyroid imaging. Nucl Med Commun 2003; 24: 111-3.
6. Even-Sapir E, Keidar Z, Sachs J et al. The new technology of combined transmission and emission tomography in evaluation of endocrine neoplasms. J Nucl Med 2001; 42: 998-1004.
7. Giordano A, Rubello D, Casara D. New trends in parathyroid scintigraphy. Eur J Nucl Med 2001; 28: 1409-20.
8. Gotway MB, Reddy GP, Webb WR et al. Comparison between MR imaging and ^{99m}Tc MIBI scintigraphy in the evaluation of recurrent of persistent hyperparathyroidism. Radiology 2001; 218: 783-90.
9. Hetrakul N, Civelek AC, Stagg CA et al. In vitro accumulation of technetium-99m-sestamibi in human parathyroid mitochondria. Surgery 2001; 130: 1011-8.
10. Hosten N, Lemke AJ, Wiedenmann B et al. Combined imaging techniques for pancreatic cancer. Lancet 2000; 356(9233): 909-10.
11. Hosten N, Kreissig R, Puls R et al. Fusion von CT- und PET-Daten: Methoden und klinische Bedeutung am Beispiel der Planung der laserinduzierten Thermotherapie von Lebermetastasen. Röfo Fortschr Geb Röntgenstr Neuen Bildgeb Verfahr 2000; 172: 630-5.
12. Ishibashi M, Nishida H, Hiromatsu Y et al. Localization of ectopic parathyroid glands using technetium-99m sestamibi imaging: comparison with magnetic resonance and computed tomographic imaging. Eur J Nucl Med 1997; 24: 197-201.
13. Israel O, Keidar Z, Iosilevsky G et al. The fusion of anatomic and physiologic imaging in the management of patients with cancer. Semin Nucl Med 2001; 31: 191-205.
14. Kaczirek K, Prager G, Kienast O et al. Combined transmission and ^{99m}Tc-sestamibi emission tomography for localization of mediastinal parathyroid glands. Nuklearmedizin 2003; 42: 220-3.
15. Krausz Y, Lebensart PD, Klein M et al. Preoperative localization of parathyroid adenoma in patients with concomitant thyroid nodular disease. World J Surg 2000; 24: 1573-8.
16. Kumar A, Cozens NJ, Nash JR. Sestamibi scan-directed unilateral neck exploration for primary hyperparathyroidism due to a solitary adenoma. Eur J Surg Oncol 2000; 26: 785-8.
17. Lee VS, Spritzer CE, Coleman RE et al. The complementary roles of fast spin-echo MR imaging and double-phase ^{99m}Tc-sestamibi scintigraphy for localization of hyperfunctioning parathyroid glands. AJR Am J Roentgenol 1996; 167: 1555-62.
18. Lopez Hänninen E, Vogl TJ, Steinmüller T et al. Preoperative contrast-enhanced MRI of the parathyroid glands in hyperparathyroidism. Invest Radiol 2000; 35: 426-30.
19. Maes F, Collignon A, Vandermeulen D et al. Multimodality image registration by maximization of mutual information. IEEE Trans Med Imaging 1997; 16: 187-98.
20. Maintz JB, Viergever MA. A survey of medical image registration. Med Image Anal 1998; 2: 1-36.
21. Marx SJ. Hyperparathyroid and hypoparathyroid disorders. N Engl J Med 2000; 343: 1863-75.
22. Mazzeo S, Caramella D, Lencioni R et al. Comparison among sonography, double-tracer subtraction scintigraphy, and double-phase scintigraphy in the detection of parathyroid lesions. Am J Roentgenol 1996; 166: 1465-70.
23. Moka D, Voth E, Larena-Avellaneda A et al. ^{99m}Tc-MIBI-SPECT-Nebenschilddrüsenszintigraphie zur präoperativen Lokalisation kleiner Nebenschilddrüsenadenome. Nuklearmedizin 1997; 36: 240-4.
24. Moka D, Voth E, Dietlein M et al. Technetium-^{99m}-MIBI-SPECT: A highly sensitive diagnostic tool for localization of parathyroid adenomas. Surgery 2000; 128: 29-35.
25. Moka D, Voth E, Dietlein M et al. Preoperative localization of parathyroid adenomas using 99mTc-MIBI scintigraphy. Am J Med 2000; 108: 733-6.
26. Perrier ND, Ituarte PH, Morita E et al. Parathyroid surgery: separating promise from reality. J Clin Endocrinol Metab 2002; 87: 1024-9.
27. Pluim JP, Maintz JB, Viergever MA. Image registration by maximization of combined mutual information and gradient information. IEEE Trans Med Imaging 2000; 19: 809-14.
28. Pons F, Torregrosa V, Fuster D. Biological factors influencing parathyroid localization. Nucl Med Commun 2003; 24: 121-4.
29. Prager G, Czerny C, Kurtaran A et al. Der Stellenwert präoperativer Lokalisationsmethoden beim primären Hyperparathyreoidismus. Chirurg 1999: 70: 1082-8.
30. Rohlfing T, Beier J. Improving reliability and performance of voxel-based registration by coincidence thresholding and volume clipping. In: Hawkes DJ, Hill DLG, Gaston R (eds). Proceedings of medical image understanding and analysis. London: Kings College 1999, 165-8.
31. Rubello D, Casara D, Fiore D et al. An ectopic mediastinal parathyroid adenoma accurately located by a single-day imaging protocol of Tc-99m pertechnetate-MIBI subtraction scintigraphy and MIBI-SPECT-computed tomographic image fusion. Clin Nucl Med 2002; 27: 186-90.
32. Russell CF, Edis AJ. Surgery for primary hyperparathyroidism: experience with 500 consecutive cases and evaluation of the role of surgery in the asymptomatic patient. Br J Surg 1982; 69: 244-7.
33. Scheiner JD, Dupuy DE, Monchik JM et al. Preoperative localization of parathyroid adenomas: a comparison of power and colour Doppler ultrasonography with nuclear medicine scintigraphy. Clin Radiol 2001; 56: 984-8.
34. Staudenherz A, Abela C, Niederle B et al. Comparison and histopathological correlation of three parathyroid imaging methods in a population with a high prevalence of concomitant thyroid diseases. Eur J Nucl Med 1997; 24: 143-9.
35. Takebayashi S, Hidai H, Chiba T et al. Hyperfunctional parathyroid glands with ^{99m}Tc-MIBI scan: semiquantitative analysis correlated with histologic findings. J Nucl Med 1999; 40: 1792-7.
36. Torregrosa JV, Fernandez-Cruz L, Canalejo A et al. ^{99m}Tc-sestamibi scintigraphy and cell cycle in parathyroid glands of secondary hyperparathyroidism. World J Surg 2000; 24: 1386-90.
37. Udelsman R. Six hundred fifty-six consecutive explorations for primary hyperparathyroidism. Ann Surg 2002; 235: 665-70.
38. Wakamatsu H, Noguchi S, Yamashita H et al. Technetium-99m tetrofosmin for parathyroid scintigraphy: a direct comparison with ^{99m}Tc-MIBI, 201Tl, MRI and US. Eur J Nucl Med 2001; 28: 1817-27.
39. Weber AL, Randolph G, Aksoy FG. The thyroid and parathyroid glands. CT and MR imaging and correlation with pathology and clinical findings. Radiol Clin North Am 2000; 38: 1105-29.
40. Weber DA, Ivanovic M. Correlative image registration. Semin Nucl Med 1994; 24: 311-23.
41. Weiss M, Benecke F, Schmid R et al. Kann durch den Einsatz der SPECT-Technik die diagnostische Aussage der präoperativen Tc-99m-MIBI-Szintigraphie beim primären Hyperparathyreoidismus verbessert werden? Med Klin 2002; 97: 389-95.
42. West J, Fitzpatrick JM, Wang MY et al. Comparison and evaluation of retrospective intermodality brain image registration techniques. J Comput Assist Tomogr 1997; 21: 554-66.

Correspondence to:
Dr. Juri Ruf
Klinik für Strahlenheilkunde, Bereich Nuklearmedizin
Charité - Universitätsmedizin Berlin
Campus Virchow-Klinikum
Augustenburger Platz 1, 13353 Berlin
Tel. +49/(0)30/4 50 55-71 27, Fax -79 09
E-Mail: juri.ruf@charite.de